ELSEVIER

Polymer 40 (1999) 5545–5552

polymer

Polymer blends of poly(ε-caprolactone) and poly(vinyl methyl ether) – thermal properties and morphology

W.Y. Yam[a], J. Ismail[a], H.W. Kammer[a,*], H. Schmidt[b], C. Kummerlöwe[b]

[a]*School of Chemical Sciences, Universiti Sains Malaysia, 11800 Penang, Malaysia*
[b]*Fachhochschule Osnabrück, Albrechtstrasse 30, D-49076 Osnabrück, Germany*

Received 2 October 1998; received in revised form 17 November 1998; accepted 17 November 1998

Abstract

We report on thermal properties and the phase behaviour of polymer blends comprising poly(ε-caprolactone) (PCL) and poly(vinyl methyl ether) (PVME). The blends were subjected to different thermal histories. In all cases, the fraction of PCL, that crystallizes in the blends, increases slightly up to 30% content of PVME. Crystallization rates of PCL are found markedly reduced in blends as compared to neat PCL. Ring-banded spherulites develop during isothermal crystallization. Radial growth rates of spherulites decrease exponentially with increasing PVME content up to approximately 40% of PVME. At higher PVME contents non-exponential decrease was observed. Melting points of PCL in blends were determined applying a step-wise annealing procedure. The glass transition temperatures of the blends reveal formation of PVME-rich phases even after rapid quenching of the homogeneous melt owing to crystallization of PCL. Lower critical solution temperature behaviour of the melts could be determined tentatively by optical inspection. The homogeneous melt phase-separates above approximately 190°C.

Keywords: Poly(ε-caprolactone); Poly(vinyl methyl ether); Polymer blend

1. Introduction

Polymer blends, comprising as one constituent poly(ε-caprolactone) (PCL), have been studied extensively in recent years. It turned out that PCL is miscible on a molecular scale in the melt with various polymers, e.g., with poly(vinyl chloride) [1,2], chlorinated polyethylenes [3], poly(styrene-co-acrylonitrile) (SAN) [4,5], poly(vinyl methyl ether) (PVME) [6,7]. In some cases, LCST (lower critical solution temperature) behaviour was observed. Also at sufficiently low temperatures, the blends start to phase separate owing to crystallization of PCL. Moreover, there is experimental evidence that in PCL/SAN blends a virtual UCST (upper critical solution temperature) exists where liquid–liquid phase separation advances prior to crystallization [8]. In any case, neat PCL lamellae are growing below the melting temperature of PCL and the blend separates into different phases, the crystalline phase comprising only PCL and an amorphous mixture of both constituents. Usually, the morphologies that develop are rather complex. One observes intra- as well as interspherulitic segregation of the amorphous phase.

The presence of an amorphous component strongly influences the crystallization behaviour of PCL and the resulting morphology [9,10]. Near the growing crystallites, the amorphous phase locally depletes of PCL. The resulting concentration gradient causes diffusion of PCL chains towards the growing front of the crystallites. This diffusion, however, is hindered by the amorphous component leading to a slowing down of the overall rate of crystallization with increasing content of the amorphous component in the blend. Moreover, the difference between crystallization temperature, T_c, and glass transition temperature, T_g, of the amorphous phase affects the crystallization process. If the amorphous component has a T_g higher than T_c, depletion of PCL near the growing crystallites leads locally to an increasing glass transition temperature of the amorphous phase which affects also the diffusion of the PCL chains and results in less perfectly crystallized domains with increasing content of amorphous polymer in the blend. For a blend comprising an amorphous polymer with a glass transition temperature situated in between the T_g of PCL and its crystallization temperature, we have again a local increase in T_g during crystallization, however, as long as $T_g < T_c$, the amorphous regions remain mobile and may not strongly affect the

* Corresponding author. Tel.: +60-4-6577888-4032; fax: +60-4-6574854.
E-mail address: hwk@usm.my (H.W. Kammer)

0032-3861/99/$ - see front matter
PII: S0032-3861(98)00807-6

Table 1
Characteristics of the polymers

Polymer	M_w (kg/mol)	M_w/M_n	T_g[a] (°C)	T_m[b] (°C)
PCL	65	1.53	− 64	73
PCL[c]	40.4	2.61		
PVME	81.8	1.71	− 25	—

[a] Glass transition temperature.
[b] Melting temperature.
[c] Only for radial growth rates of spherulites.

perfectness of the crystallites. The latter situation, is met with in blends of PCL and PVME. Then, it might be interesting to crystallize PCL at a temperature intermediate between the glass transition temperatures of the constituents. PCL is still mobile but, PVME is not. This should result in a PVME rich amorphous phase.

In order to study crystallization and melting behaviour of these blends, samples were isothermally crystallized at different temperatures. Moreover, the blends were subjected to different thermal histories. The resulting glass transition temperatures were determined by differential scanning calorimetry. Morphologies and phase behaviour of the blends were studied by optical microscopy.

2. Experimental

2.1. Polymers

PCL and PVME were commercial products provided by Aldrich and BASF, respectively. The polymers were used as received. Only for determination of the radial growth rates of spherulites, PCLs with two different molecular masses were applied. Molecular weight data are listed in Table 1.

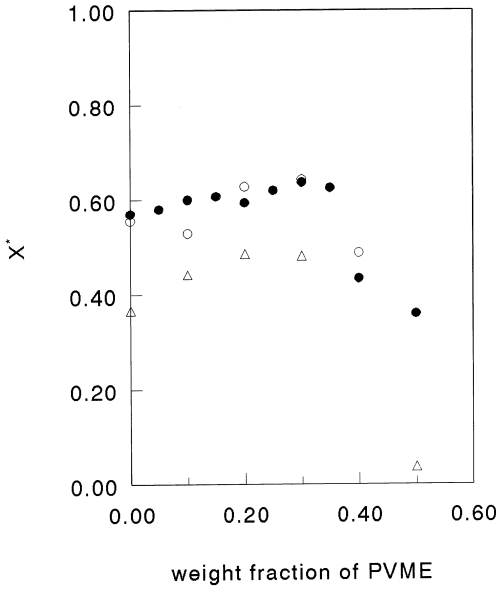

Fig. 1. Crystallinity X^* of PCL, that developed during different thermal procedures, versus blend composition (○) thermal history *I*, $T_c = 40$°C, (△) thermal history *II*, (●) thermal history *III*.

2.2. Blend preparation

Stock solutions of the individual polymers were prepared by dissolving them in toluene at a polymer concentration of 5% by weight. For formation of PCL/PVME blends, appropriate amounts of the stock solutions were mixed and cast on glass plates. The solvent was evaporated under vacuum at 80°C for several days.

2.3. Techniques

Melting and crystallization behaviour as well as the glass transition temperature of the blends were studied by DSC using a Perkin-Elmer DSC-7. Optical microscopy, using a Zeiss polarizing microscope equipped with a Linkam heating/cooling unit (Linkam TM 600/s), was employed for studies of blend morphologies and tentative phase behaviour in the melt.

The samples were exposed to different thermal histories:

I. Isothermal crystallization experiments
Samples were annealed for 10 min at 95°C followed by rapid cooling at a rate of −200°C/min to the respective crystallization temperatures near 40°C. Then, samples were crystallized at T_c for a period of time $t_c = 5t_{0.5}$ with $t_{0.5}$ being the corresponding half-time of crystallization where 50% of the material was crystallized. In the isothermal crystallization experiments, crystallinity was expressed as the ratio of peak areas at time t to that at the end of crystallization. Afterwards, the corresponding melting temperatures were determined by heating the blends with a rate of 20°C/min to 20 K above the melting temperature.

II. Rapid quenching from the melt
The blends were annealed at 95°C for 10 min, then rapidly cooled (rate: −200°C/min) to −75°C. Afterwards, the DSC scan was carried out with a rate of 20°C/min.

III. Annealing at −40°C
After annealing at 95°C for 10 min, the blends were rapidly cooled to −40°C, there annealed for 1 h followed by rapid cooling to −75°C and again, the DSC scan was taken with 20°C/min.

The degree of crystallinity of PCL in the blends at low temperatures (at around −75°C), X^*, was estimated from the difference in the experimentally determined melting and cold crystallization enthalpies, ΔH, and the reference melting enthalpy of 100% crystalline PCL, ΔH_{ref}, via $X^* = \Delta H/(w_{PCL}\Delta H_{ref})$ where w_{PCL} is the weight fraction of PCL and $\Delta H_{ref} = 136.1$ J/g [1].

The inflection points of the heat flow curves were taken as the glass transitions.

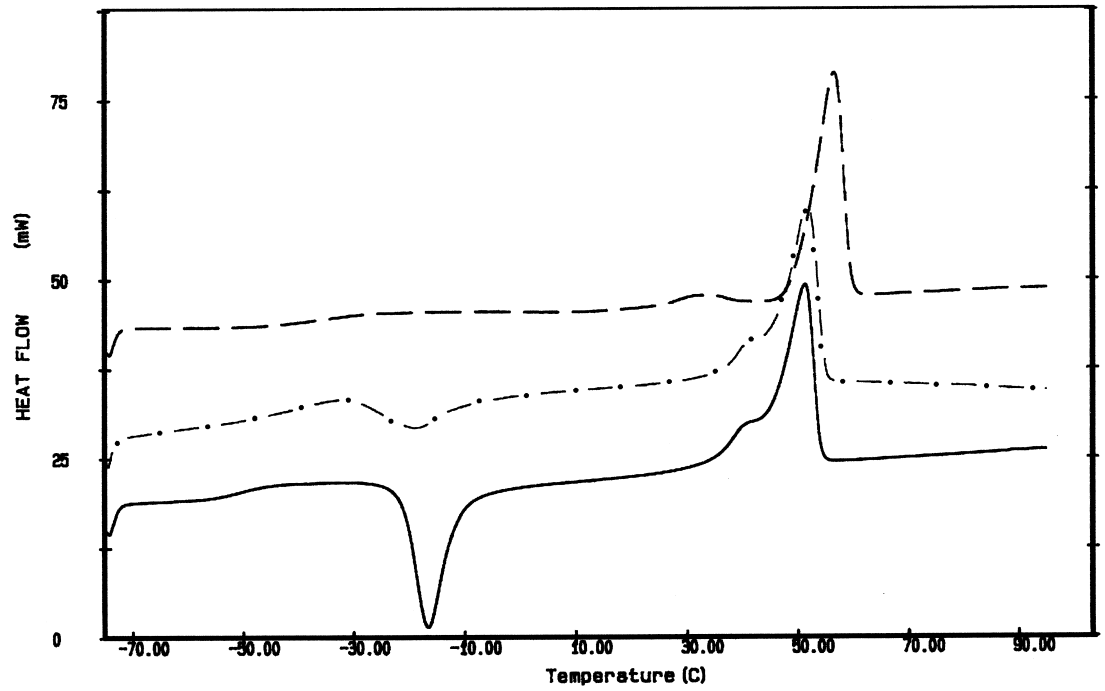

Fig. 2. DSC traces of reheating cycles for the PCL/PVME 60/40 blend after exposing it to the thermal histories *I–III*. *I* – dashed curve, $T_c = 42°C$, *II* – solid curve, *III* – dash-dotted curve.

2.4. Measurement of spherulite growth rates

Each sample was heated up to 80°C. This temperature was held for 5 min, and then the samples were cooled with 50°C/min to the crystallization temperature of 40°C. The spherulite diameters were determined photographically as a function of time.

2.5. Determination of LCST

The phase separation temperatures were detected by optical microscopy. The blends were heated above 180°C with a rate of 1°C/min under nitrogen atmosphere to avoid thermal degradation.

3. Results and discussion

3.1. Crystallization and melting behaviour

The PCL/PVME blends were exposed to different thermal procedures: I – isothermal crystallization at temperatures from 37°C–48°C, II – quenching from the melt, and III – annealing at −40°C, a temperature between the glass transition temperatures of the blend components. The PCL crystallinities, *X**, that developed in the course of the different thermal procedures, are shown in Fig. 1 as a function of PVME content in the blend. The crystallinity of pure PCL reaches a value of about 57% during isothermal crystallization as well as during the annealing process at −40°C. Rapid quenching cannot prevent crystallization of PCL, but, the crystallinity is significantly lowered (37%). The crystallinity *X** increases up to a PVME content of about 30 wt%. In blends with PVME in excess, PCL crystallization is hindered. The PCL crystallinity does not change significantly when PCL is crystallized isothermally at different temperatures (regime *I*).

In blends with 40 wt% PVME and more, cold crystallization peaks during reheating of samples after thermal histories II and III can be observed in the DSC scans. A typical example is shown in Fig. 2 for the PCL/PVME 60/40 blend. Only one melting peak at 56.6°C can be seen after isothermal crystallization (*I*). PCL exhibits a crystallinity *X** of about 60% during the isothermal crystallization process. Crystallization is nearly impeded in PCL/PVME 60/40 blends during rapid quenching from the melt (*II*). After quenching, the reheating trace shows a cold crystallization peak with an enthalpy approximately equal to that of the following melting peak. The heating scan *III* obtained after annealing the 60/40 blend at −40°C displays a cold crystallization peak and a remarkable larger melting peak. This suggests that most of the crystallinity developed during annealing at −40°C. The glass transitions indicated in Fig. 2 will be discussed later.

3.2. Kinetics of isothermal crystallization

Overall kinetics of crystallization was analysed in terms of Avrami equation [11]

$$X(t) = 1 - \exp\left[-K_A(t - t_0)^{n_A}\right]$$

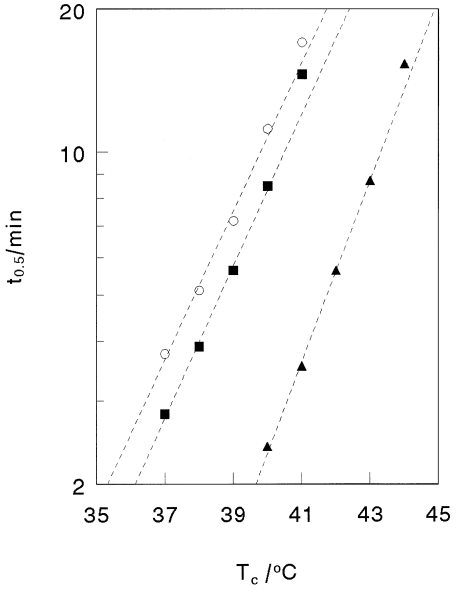

Fig. 3. Half-time of crystallization versus crystallization temperature for PCL in PCL/PVME blends, (▲) 100/0, (■) 90/10, (○) 70/30.

where X(t) is defined as the ratio of degree of crystallinity at time t and the final degree of crystallinity; $X(t)$, ratio of peak areas $a(t)/a(\infty)$,was normalized so as to take unity at $t \rightarrow \infty$. The quantities K_A and n_A are the overall rate constant of crystallization and the Avrami exponent, respectively; t_0 represents the induction period which was determined experimentally and defined as the time where approximately 1% of crystallinity was measured.

In order to impose comparable thermal histories to semicrystalline blends, isothermal crystallization experiments require determination of the half-time of crystallization, $t_{0.5}$, defined as the time taken for half of the crystallinity to develop. Quantities $t_{0.5}$ were estimated from the area of the crystallization peak at the respective crystallization temperature, T_c. Fig. 3 shows semilogarithmic plots of half-times of crystallization versus the crystallization

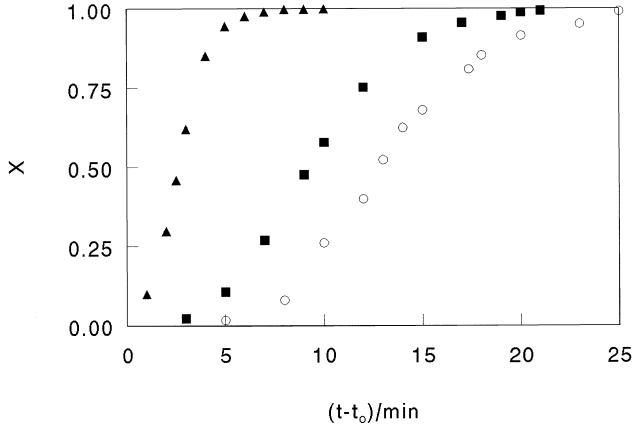

Fig. 4. Normalized crystallinity, X, versus crystallization time for PCL in PCL/PVME blends at 40°C. Markers as in Fig. 3.

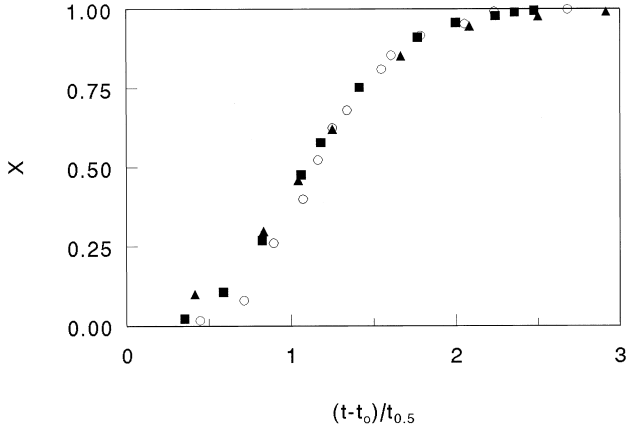

Fig. 5. Crystallinity versus reduced time $(t - t_0)/t_{0.5}$ for PCL in blends of PCL/PVME, $T_c = 40$°C. Markers as in Fig. 3.

temperature. In a certain range of crystallization temperatures, the half-times increase exponentially with temperature. At sufficiently high crystallization temperatures, deviations from exponential behaviour may occur. The half-times also increase with ascending content of PVME in the blends.

The blends were treated according to the procedure I described in the experimental section 2. Fig. 4 shows the normalized crystallinity, X, as a function of time $(t - t_0)$ for PCL blends crystallized at 40°C. The growing rate slows down with increasing PVME content. The different curves coincide and form a master curve to a good approximation when X is plotted against the reduced time $(t - t_0)/t_{0.5}$ (Fig. 5). This indicates that overall features of crystallization do not significantly change with composition in PCL/PVME

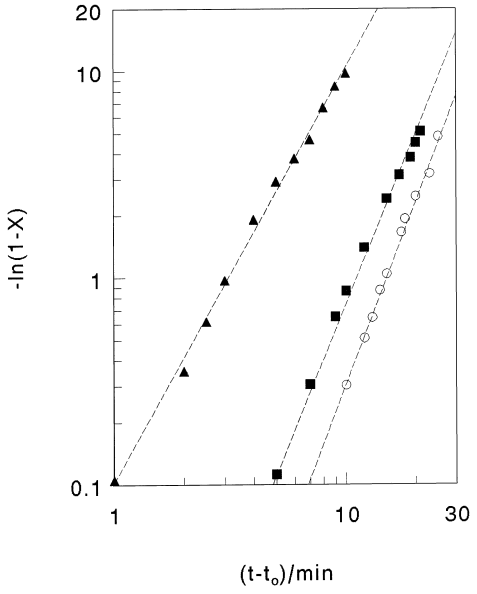

Fig. 6. Avrami plots for PCL/PVME blends, $T_c = 40$°C. Markers as in Fig. 3.

Table 2
Avrami parameters for the kinetics of crystallization in PCL/PVME blends at 40°C

Blend	n_A	$10^2 K_A$ (min^{-nA})	t_0 (min)	$t_{0.5}$ (min)	r^a
100/0	2.01	10.2	0.25	2.40	0.998
90/10	2.75	0.13	0.75	8.48	0.997
80/20	2.69	0.096	2.68	8.92	0.999
70/30	2.93	0.036	4.08	11.19	0.998

[a] Correlation coefficient.

blends. Fig. 6 gives examples of Avrami plots. Linear relationships can be seen up to high degrees of conversion. Parameters estimated from the plots are summarized in Table 2. Avrami exponents are relatively close to 3 and there are only minor changes of the Avrami exponent with blend composition.

3.3. Spherulite growth rates

The radial growth rate of PCL spherulites was determined by optical microscopy at a crystallization temperature of 40°C. Two different PCLs with molecular masses of 40 400 and 65 000 were used as blend components. The spherulite radii increase strictly linearly with time for all blends. The radial growth rates, plotted in Fig. 7 as a function of blend composition, were calculated from the slope of radius versus time plots. As expected, the radial growth rate decreases with increasing molecular mass of PCL. Moreover if PCL is in excess, the radial growth rate decreases exponentially with increasing PVME content in the blend. At sufficiently high PVME content, however, non-exponential decrease of the growth rate can be seen. These deviations from exponential behaviour become more pronounced in blends with PCL of the lower molecular mass.

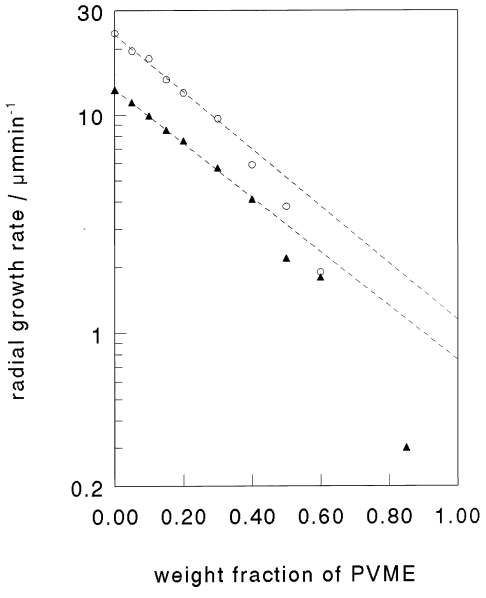

Fig. 7. Radial growth rate of PCL spherulites versus blend composition, $T_c = 40$°C. (○) PCL $M_w = 40\,400$, (▲) PCL $M_w = 65\,000$.

It might be interesting to compare qualitatively the radial growth rates in PCL/PVME (PCL, $M_w = 40\,400$) with previous results on growth rates in blends of PCL and poly(-styrene-ran-acrylonitrile) (SAN-*x*; *x* denotes the AN content of the copolymer in wt%) [12]. In 50/50 blends of PCL with SAN-22.7 and SAN-12.9, the growth rates amount to 0.23 and 1.24 μm/min, respectively, at $T_c = 40$°C, whereas the PCL/PVME 50/50 blend exhibits a growth rate of 3.8 μm/min. These results suggest that two effects influence the radial growth rate of PCL spherulites from a mixed melt: the thermodynamic stability of the mixture and the difference in glass transition temperature of the amorphous constituents and the crystallization temperature. The glass transition temperature of the SAN copolymers is much higher than the crystallization temperature of PCL while in blends with PVME, the glass transition temperatures of both the amorphous mixture and PVME are lower than T_c. Therefore, the rates are lower in the PCL/SAN-*x* blends than in the PCL/PVME blend. On the contrary, the remarkable difference in the growing rates between blends with SAN-22.7 and SAN-12.9 results from the different thermodynamic stability of the mixtures. The PCL/SAN-12.9 blend is situated at the edge of the miscibility window while the blend with SAN-22.9 is almost in the centre of that window [5].

3.4. Melting behaviour

A step-wise annealing procedure after Hoffman and Weeks [13] was employed to estimate the equilibrium melting temperatures of the blends under discussion. The blends were treated according to the procedure I described in the experimental section (Section 2). After isothermal crystallization, melting points were detected by heating the samples with a speed of 20 K/min. The DSC scans of all samples displayed only one endotherm. Hoffman–Weeks plots of PCL/PVME blends are presented in Fig. 8, and the results of linear regressions are summarized in Table 3. There is no systematic variation of the melting point with blend composition.

3.5. Glass transition temperatures

The PCL/PVME blends were exposed to the procedures II and III, described in the experimental section (Section 2), in order to determine the glass transition temperatures, T_g, and to study the influence of crystallization on them. Results are shown in Figs. 9 and 10. As discussed before, rapid quenching of the blends from the melt cannot prevent crystallization of PCL, however, the final degree of crystallinity is reduced as compared to isothermal crystallization and annealing (see Fig. 1). The glass transition temperatures of the quenched blends decrease with decreasing PVME content. One recognizes, however, that the decrease in T_g with descending content of PVME is not as large as one

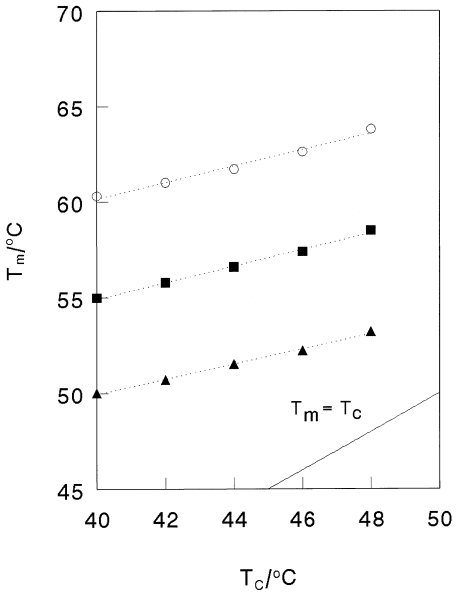

Fig. 8. Hoffman–Weeks plots for PCL in PCL/PVME blends. Markers as in Fig. 3. 70/30 blend – original position; 90/10 and 100/0 displaced by − 5°C and − 10°C, respectively.

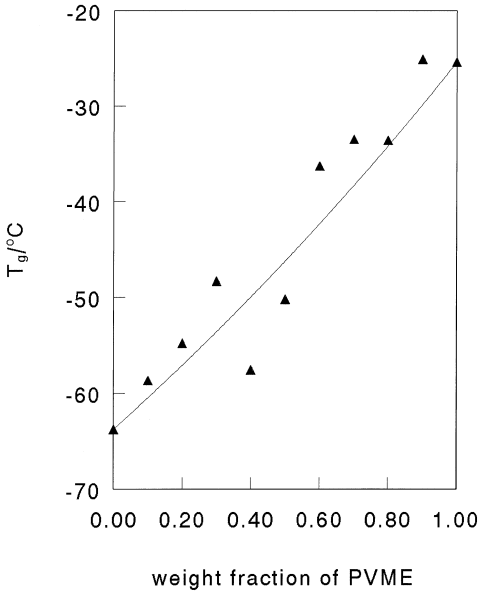

Fig. 9. Midpoint T_g as a function of PVME content in blends of PCL and PVME. Blends were subjected to thermal history II (cf. text). The solid curve was calculated according to Fox equation.

expects for a completely miscible system. This indicates that a PVME-rich phase exists even in blends comprising 30 wt % and less PVME. Fig. 1 shows that the degree of crystallinity in 60/40 and 50/50 PCL/PVME blends is very low after rapid cooling. Crystallization in these blends started only above −25°C (cf. Fig. 2). It is likely that the glass transition temperatures for these blends, shown in Fig. 9, are attributed to PCL-rich phases.

The situation changes for thermal history III, Fig. 10. Similar glass transitions as for the quenched blends can be found only for blends with more than approximately 60 wt% PVME, as in that range, the applied annealing temperature, −40°C, is lower than the glass transition of the amorphous mixture. Therefore, crystallization of PCL cannot proceed during annealing at −40°C. For blends with less than 60% PVME, the annealing temperature is higher than the glass transition. The chains are mobile enough and crystallization continues during annealing time. This leads to higher crystallinity of PCL in the blend as shown in Figs. 1 and 2. Concomitantly, one observes large deviations of the glass transition temperature from the Fox equation. The glass transition temperatures of blends with high PCL content, between 95 and 50 wt%, change only slightly with blend composition. One may conclude that a PVME-rich phase develops during the annealing process. The glass transition temperatures of that phase indicate a composition of 50–70 wt% PVME according to the Fox equation. Similar effects might be recognized in blends crystallized isothermally near 40°C. Glass transitions of the PCL/PVME 60/40 blend are indicated in Fig. 2. The T_g's of the isothermally crystallized sample (I) and of the sample annealed at −40°C (III) appear in the same region. This indicates again the formation of a PVME-rich amorphous phase during

Table 3
Apparent equilibrium melting points T_m^0 and correlation coefficients of the T_m vs. T_c relationships in the range 40°C–48°C for the crystallization temperature T_c

Blend PCL/PVME	T_m^0 (°C)	r
100/0	73	0.998
90/10	75	0.998
80/20	78	0.997
70/30	75	0.993

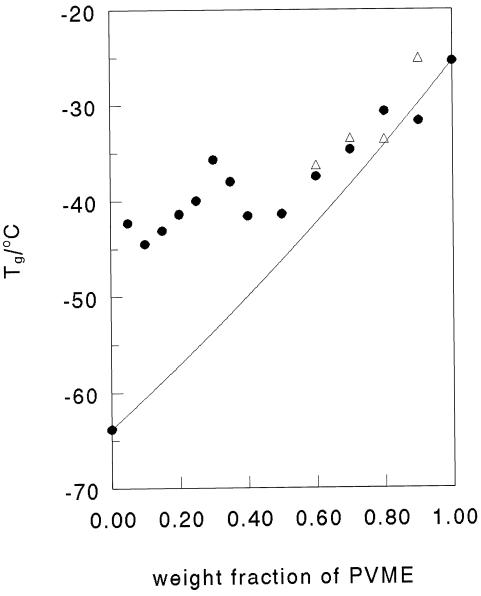

Fig. 10. As Fig. 9 for thermal history III (cf. text). The open triangles represent data points of Fig. 9, for comparison.

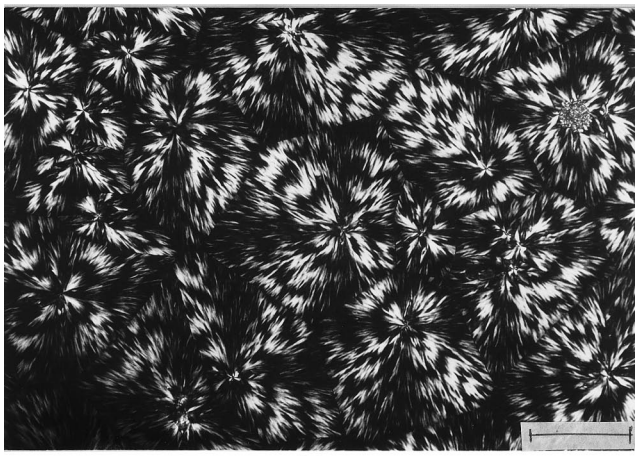

Fig. 11. Spherulite morphology of PCL/PVME blends, crystallized from the melt at 40°C, obtained by optical microscopy with crossed polars. (a) 90/10, (b) 50/50. Bars correspond to 100 μm.

isothermal crystallization at temperatures well above the glass transition.

From the T_g data presented, one may conclude that PVME-rich amorphous and PCL-rich semicrystalline phases are formed in PCL/PVME blends when the blends are allowed to crystallize at temperatures above the glass transition of the amorphous melt. The extent of miscibility of PVME and PCL in amorphous regions is strongly influenced by the crystallization conditions.

3.6. Blend morphologies and phase behaviour

Fig. 11 shows selected examples of spherulite morphologies that developed in blends of PCL and PVME after isothermal crystallization at 40°C. A fibrillar fine texture of the spherulites as well as distinct ring-shaped structures can be seen. Spherulites exhibiting ring-banded patterns have been observed in various miscible PCL-based blends, e.g. in PCL/PVC [1,2,14–17] or in PCL/SAN blends [9,12,18]. The ring-banded spherulites in PCL/PVME blends are very similar to those observed in PCL/SAN blends [12].

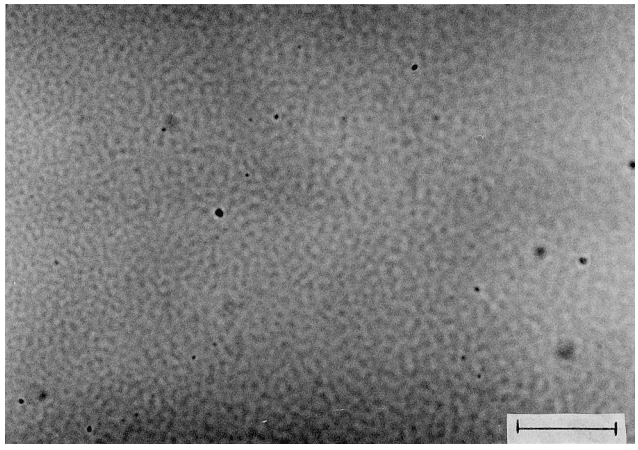

Fig. 12. Optical micrograph of spinodal decomposition patterns for a 50/50 PCL/PVME blend at 192°C. The blend was heated with a rate of 1°C/min from 180°C–193°C. Bar corresponds to 100 μm.

The phase behaviour of PCL/PVME blends in the molten state was estimated tentatively by optical inspection in the hot stage. Samples were heated above 180°C by a rate of 1°C/min. The temperatures, where regular spinodal decomposition patterns occurred, were taken as the phase separation temperatures. One typical example is shown in Fig. 12. In that way, we could succeed only with three blends to detect the phase separation temperatures (Fig. 13). The experimental data points were used to estimate the free-energy parameter X given by [19]

$$X = \frac{\tilde{V}_A^{1/3}}{\tilde{V}_A^{1/3} - 1} 2X_{AB} + \frac{\tilde{V}_A^{1/3}}{(4/3) - \tilde{V}_A^{1/3}} \frac{7}{8} \Gamma^2 \quad (1)$$

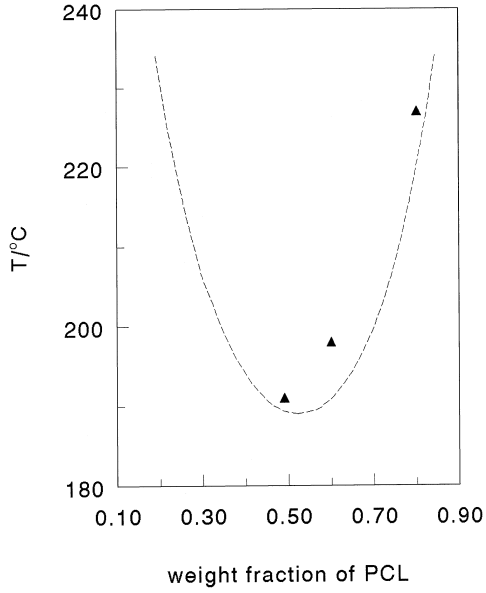

Fig. 13. Binodal for the system PCL/PVME. Markers indicate experimental data points. The curve was calculated according to Flory–Huggins theory (see text).

where $\tilde{V}_A$ is the reduced volume of the reference component, X_{AB} and Γ are the interaction and free-volume parameter, respectively. With the experimental data points indicated in Fig. 13 and using PCL with $T_A^* = 7200$ K as the reference component, one gets for the two parameters in Eq. (1)

$$X_{AB} = -8 \times 10^{-5} \qquad \text{and} \qquad \Gamma^2 = 0.0013 \tag{2}$$

It turns out that the segmental interaction parameter X_{AB} is extremely small in blends of PCL and PVME. The binodal, indicated in Fig. 13, was calculated on the basis of the Flory–Huggins equation with the free-energy parameter (1), parameters of Eq. (2) and the polymerization indices $r_{PC} = 570$, $r_{PVME} = 690$.

In conclusion, blends of PCL and PVME exhibit LCST behaviour with a critical temperature at approximately 190°C. Below that temperature, the melt is homogeneous. In blends with PCL in excess, crystallization of PCL cannot be suppressed not even during rapid quenching. This results in the formation of PVME-rich phases. Ring-banded spherulites develop during isothermal crystallization. The radial growth rate of spherulites decreases exponentially with increasing PVME content as long as PCL is in excess. Non-exponential decrease of the growth rate occurs at even higher PVME contents.

Acknowledgements

W.Y.Y., J.I. and H.W.K. are indebted to Universiti Sains Malaysia at Penang for the research grant supporting this study.

References

[1] Khambatta FB, Warner F, Russel T, Stein RS. J Polym Sci Polym Phys Ed 1976;14:1391.
[2] Ong CJ, Price FP. J Polym Sci Polym Symp 1978;63:45.
[3] Defieuw G, Groeninckx G, Reynaers H. Polymer 1989;30:595.
[4] Chiu SC, Smith TG. J Appl Polym Sci 1984;29:1797.
[5] Schulze K, Kressler J, Kammer HW. Polymer 1993;34:3704.
[6] Oudhuis AACM, Thiewes HJ, van Hutten PF, ten Brinke G. Polymer 1994;35:3936.
[7] Luyten MC, Boegels EJF, Alberda van Ekenstein GOR, ten Brinke G, Bras W, Komanschek BE, Ryan AJ. Polymer 1997;38:509.
[8] Svoboda P, Kressler J, Chiba T, Inoue T, Kammer HW. Macromolecules 1994;27:1154.
[9] Kressler J, Kammer HW, Silvestre C, DiPace E, Cimmino S, Martuscelli E. Polym Networks Blends 1991;1:225.
[10] Kammer HW, Kummerlöwe C. Adv Polym Blends Alloys Techn, 5. Lancaster, PA: Technomic Publ, 1994 :132.
[11] Mandelkern L. Crystallization of Polymers. New York: McGraw Hill, 1964.
[12] Kummerlöwe C, Kammer HW. Polym Networks Blends 1995;5:131.
[13] Hoffman JD, Weeks JJ. J Res NBS 1962;A66:13.
[14] Wang TT, Nishi T. Macromolecules 1977;10:421.
[15] Russell TP, Stein RS. J Polym Sci, Polym Phys Ed 1983;21:999.
[16] Nojima S, Watanabe K, Zheng Z, Ashida T. Polymer J Tokyo 1986;18:451.
[17] Defieuw G, Groeninckx G, Reynaers H. Polym Commun 1989;30:267.
[18] Li W, Jan R, Jiang B. Polymer 1992;33:889.
[19] Kammer HW, Kressler J, Kummerlöwe C. Adv Polym Sci 1993;106:31.